

RESEARCH

On the duration of face-to-face contacts

Stéphane Plaszczynski^{1,2*}, Gilberto Nakamura³, Basile Grammaticos^{1,2} and Mathilde Badoual^{1,2}**Abstract**

The analysis of social networks, in particular those describing face-to-face interactions between individuals, is complex due to the intertwining of the topological and temporal aspects. We revisit here both, using public data recorded by the *sociopatterns* wearable sensors in some very different sociological environments, putting particular emphasis on the contact duration timelines. As well known, the distribution of the contact duration for all the interactions within a group is broad, with tails that resemble each other, but not precisely, in different contexts. By separating each interacting pair, we find that the *fluctuations* of the contact duration around the mean-interaction time follow however a very similar pattern. This common robust behavior is observed on 7 different datasets. It suggests that, although the set of persons we interact with and the mean-time spent together, depend strongly on the environment, our tendency to allocate more or less time than usual with a given individual is invariant, i.e. governed by some rules that lie outside the social context. Additional data reveal the same fluctuations in a baboon population. This new metric, which we call the relation “contrast”, can be used to build and test agent-based models, or as an input for describing long duration contacts in epidemiological studies.

Keywords: social networks; face to face interactions; data analysis

Introduction

Since the advent of the Internet, the quantity of digital data describing our behavior has inflated, offering to scientists an unprecedented opportunity to study human interactions in a more quantitative way. This

opened the field of sociology to data-analysis and from the hard-science community, came the tacit idea that several aspects of the complex human behavior can be modeled [1, 2, 3, 4, 5, 6]. With the rapid development of mobile technologies (GPS, Bluetooth, cellphones) a lot of effort was first put in trying to capture the patterns of human mobility (for a review, see [7]). A more local picture of our everyday social interactions can be obtained using dedicated proximity sensors. Following a pioneering experiment that equipped conference participants with pocket switched devices [8, 9], the *sociopatterns* collaboration (www.sociopatterns.org) developed some wearable sensors that allow to register the complex patterns of face-to-face interactions [10, 11]. The radio-frequency signal is only recorded if two individual are in front of each other for a duration of a least 20 s (which is the timing resolution). We note that, from a sociological point of view, a distance below 1.5 m covers the traditional *private* (< 50 cm), *personal* (<1.2 m) and *social* (< 3.5 m) zones. The goal is not only to analyze social interactions but also to understand how information (or a disease) spreads over a real dynamical network [12, 13, 14, 15]. Those sensors were worn by volunteers in several work-related environments: scientific conferences [10, 13, 12], a hospital ward [16], an office [15] and at school [17, 18]. As part of a UNICEF program, they were also used to characterize social exchanges in small villages in Kenya and Malawi [19, 20] and for ethological studies on baboons [21].

It has been known for a long time that the *overall* distribution of the duration of contacts in face to face interactions is “broad” [8] and presents some “similarities” when observed in different environments (see [22] for a short review).

However, those comparisons were performed on data taken in some similar sociological environments, which are typically occidental, educated and often with a scientific background (in conferences or high-school). Here we wish to extend the study of face-to-face interactions by comparing them to some very different datasets that were originally designed for other aims. The first one are the data taken in the rural Malawi village. The second one concerns interactions among baboons in a primatology center.

Moreover, there is more information in the data than what was previously presented [10, 11]. Indeed, one

*Correspondence: stephane.plaszczynski@ijclab.in2p3.fr

¹Université Paris-Saclay, CNRS/IN2P3, IJCLab, 91405, Orsay, France

²Université Paris-Cité, IJCLab, 91405, Orsay, France

Full list of author information is available at the end of the article

has access to the full timeline of interactions for *each pair* of individuals separately (what we call in the following a “relation”). This allows to study the mean-interaction time per relation and, most importantly, deviations of the contact duration from it, which reveals the underlying relation dynamics. We will show that they are surprisingly similar in all the settings.

After describing our data selection and methodological differences with some previous studies in Sect. 1, we will focus on the details of the temporal interactions in Sect. 2.2 after showing rapidly that social interactions among the participants are obviously very different in each environment. We will introduce the concept of contrast of the contact duration (deviation from the mean) and show that the distributions are extremely similar on each dataset and for each relation individually. In the Discussion part, we comment on the utility of using the robust contrast distribution in improving agent-based models, and conclude summarizing the results and highlighting some possible future extensions. Some extra information, referred to in the text, is given in the *Supplementary Information (SI)* document.

1 Material and methods

1.1 Datasets

We have chosen four datasets from the *sociopatterns* web site, sociologically most dissimilar.

- 1 *hosp*: these are early data collected over 3 days ^[1] on 75 participants in the geriatric unit of a hospital in Lyon (France) [16]. Most interactions (75%) involve nurses and patients.
- 2 *conf*: these are also some early classical data from the ACM Hypertext 2009 (www.ht2009.org) conference that involved about a hundred of participants for 3 days [13] in Torino (Italy). The audience is international with a scientific background. There exist also some data taken at another conference in Nice in 2009 (SFHH, [23]) with more participants, but we prefer to use the former which has a number of individuals comparable to the other datasets. However we have checked that we obtain similar results with the SFHH data.
- 3 *malawi*: these proximity data were taken in a small village of the district of Dowa in Malawi (Africa) where 86 participants agreed to participate for 13 (complete) days. Interestingly those data contain both extra and intra-household interactions, although we will not distinguish them here. This community consists essentially of farmers.

- 4 *baboons* Those data were taken at a CNRS Primate Center near Marseille (France) where 13 baboons were equipped with the sensors for a duration of 26 days. The goal was to study their interactions, and study how conclusions reached from data-analysis match those provided by human observation.

With that choice, we span very different sociological environments. We have also analyzed a few other datasets collected at the SFHH conference, an office and a high-school. They give similar results (results are shown in the SI) but we consider them as sociologically closer to the *conf* one. We have chosen to focus on the *sociopatterns* data since they provide a consistent set taken with the very same devices, minimizing possible sources of systematic errors.

1.2 Differences with previous studies

Previous studies considered the overall temporal properties of interactions, i.e. without differentiating the pair of people interacting. In this work we will put accent on the temporal properties of each pair separately.

Probability distribution functions (p.d.f) are often estimated by histograms, i.e. by counting the number of samples that fall within some bin. But for heavy-tailed distributions the size of the bins is delicate to choose. With a constant size binning, several bins end up empty for large values. Using a logarithmically increasing binning is neither a solution since it supposes that the distribution is constant on the wide range of last bins. Following [24], we will use instead the *probability to exceed* function (p.t.e, also known as the “complementary cumulative distribution function” or Zipf plot) which is computed simply by sorting the samples and plotting them with respect to their relative frequency. In this way, one does not need to define a binning and the distribution is easier to apprehend.

2 Results

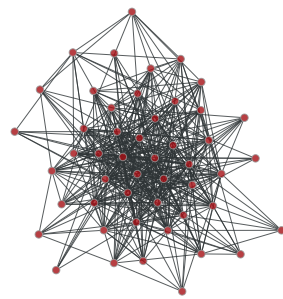
2.1 Interactions between individuals

Since it is not our primary goal to study the social structures in those very different communities, we just highlight visually some differences on Figure 1 which shows 24 hr time-aggregated graphs of the relations between individuals.

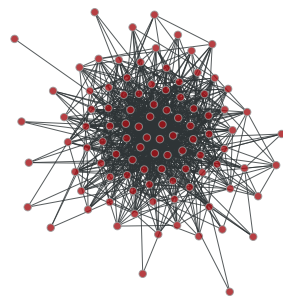
The graphs for the *hosp* and especially the *conf* datasets show a strongly connected core. The *malawi* one is much sparser, while the *baboons* one is almost complete showing that each animal interact with all the others.

Table 1 gives a more quantitative view of some of the graph’s properties. The number of different people met per day (the degree of the graphs) is about 20 in both the hospital and the conference environments.

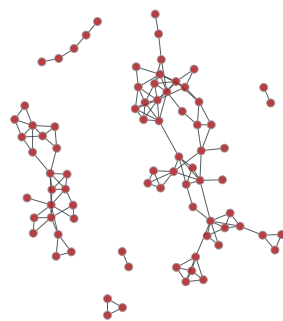
^[1]here and in the following, we will only consider complete (24 h) day periods.



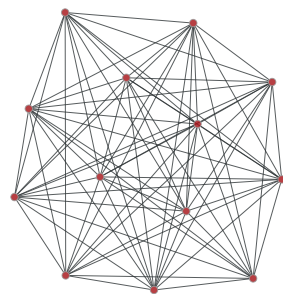
(a) hosp



(b) conf



(c) malawi



(d) baboons

Figure 1 Aggregated graphs of interactions over one day for our 4 datasets. Vertices (red points) represent agents and there is a link (edge) if there was at least one face-to-face interaction for more than 20 s. The first day from the datasets is used, but very similar results are obtained with the others.

group	T	N	$\langle k \rangle$	$\langle w \rangle$ (mins)	$\langle s \rangle$ (mins)
<i>hosp</i>	3	49 ± 1	18 ± 1	6 ± 13	97 ± 101
<i>conf</i>	3	100 ± 3	20 ± 1	2 ± 14	46 ± 63
<i>malawi</i>	12	70 ± 4	3 ± 1	24 ± 37	65 ± 74
<i>baboons</i>	26	13 ± 1	11 ± 1	8 ± 11	87 ± 53

Table 1 Properties of time aggregated graphs on each dataset per day. Uncertainties are the standard deviations between the days. T is the number of (complete) days in the dataset. N the number of interacting agents. $\langle k \rangle$ is the mean degree, i.e. the average number of agents each individual interacts with during one day. $\langle w \rangle$ is the mean weight where the weights specify the total duration of a single relation [25]. Mean strength $\langle s \rangle$ which represents the average total interaction time per individual.

As is apparent in Figure 1(c), it is much smaller in the rural community (3). But the interaction times are longer ($\simeq 25$ min) which reflect different sector of activities (agrarian and including inter-housing relations for the *malawi* data).

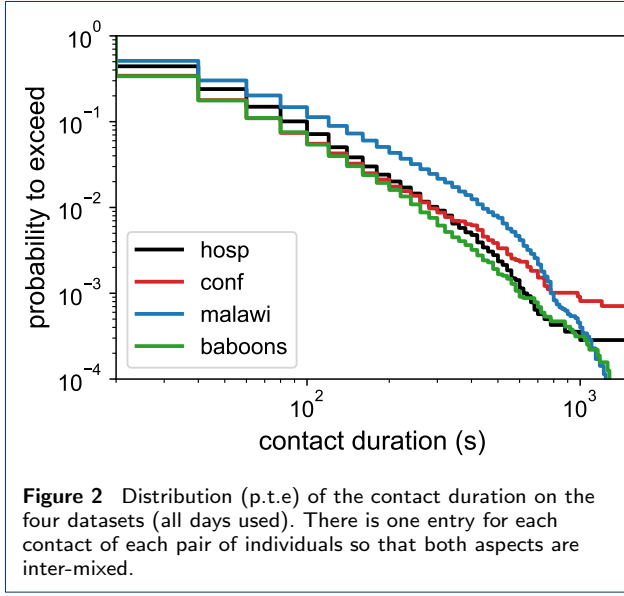
The strength of the relation represents the total time per individual spent interacting with others per day. It is essentially the product of the mean number of people met per day by the time spent interacting with them ($\langle s \rangle \simeq \langle k \rangle \langle w \rangle$). It varies by a factor of two (from 45 min to 1.5 h) although the large standard-deviations indicates important daily variations due to the heavy-tail of the distribution.

The comparison to the *baboons* dataset should be handled with care since there is a much smaller number of agents (13). Since each baboon interacts essentially with each other (Figure 1(d)), the mean degree is bounded to $\langle k \rangle \simeq N$. On the other hand, their small number possibly increases their interaction duration ($\langle w \rangle$) so that the strength of their relation is finally similar to that of the human groups.

The goal of this short section is not to dwell into the topological details of these time evolving graphs, but to illustrate that, as expected, these heterogeneous sociological groups show some very distinct interaction patterns between individuals.

2.2 Face to face temporal relations

We are interested in the duration of the contacts in those different networks. Figure 2 shows a classical distribution, that of the duration of contacts. We emphasize that such a representation mixes all the interactions of all the participants in the same plot. As well known, these distributions are “heavy-tailed”; most interactions are of short duration (at the minute level) but some may drift up to an hour. Interactions for people in *malawi* tend to last longer than for all the others. The baboons’ duration of interaction is similar to the human ones (as noticed in [21]), although there are some sizable differences at short times, somewhat squeezed by the logarithmic scale. Overall, although there is a common trend, some differences appear too.



The new aspect of this work concerns the detail of each relation separately. For a given data-taking period, each relation consists in a set of intervals measuring the beginning and end times of the interaction at the resolution of the instruments (20 s). There is a varying number of interactions (intervals) per relation, that we call $N_{int}(r)$. In the following we will consider the duration of the interactions that we note $\{t_i(r)\}_{i=1, \dots, N_{int}(r)}$. They are thus variable-size timelines expressed in units of the resolution step.

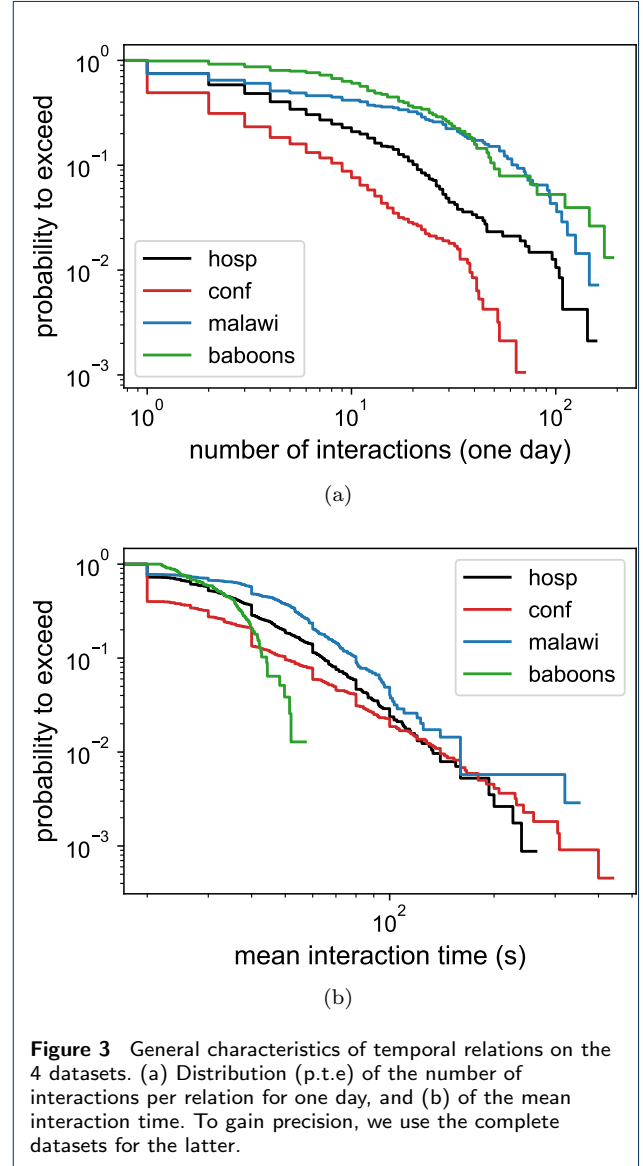
The number of registered interactions for a given pair depends on the total duration of the experiments (Table 1) but we may compare them just for one day. The distribution of this variable is shown in Figure 3(a). It is clearly different for each group. People at the conference tend to interact (with the same person) less often. In 65% of the cases it is only once per day, against 25% for the *hosp* and *malawi* datasets, and 3% for *baboons*.

The mean interaction time per relation

$$\bar{t}(r) = \frac{1}{N_{int}(r)} \sum_{i=1}^{N_{int}(r)} t_i(r), \quad (1)$$

is shown in Figure 3(b). Here again distributions are heavy-tailed and different. There is a marked difference between animals and humans, the former interacting for shorter times.

We are now interested in studying the *deviations* of the contact duration from the mean value for a given relation. Indeed, in physics the dynamics of a process is often revealed by such a quantity. For instance in cosmology, one uses the “density contrast” that represents the galactic density divided by its mean value.



It is the fundamental quantity which traces the dynamics of the underlying field (see e.g. [26]). Inspired by this example, we propose to study what we call the “duration contrast”, or simply “contrast” which is the simplest dimensionless quantity we can form to study deviations from the mean-value

$$\delta_i(r) = \frac{t_i(r)}{\bar{t}(r)}, \quad (2)$$

where r recalls that the quantity varies for each relation. The contrast represents our tendency to spend more or less time than usual with a given individual. Note that “usual” is meant as the mean-interaction time between the two peculiar agents (Figure 3) and

varies for each relation. For a small number of samples, the arithmetic mean (eq. (1)) is however a poor estimate of the true mean-time and also strongly correlated to the individual samples. Taking the ratio leads to a very noisy estimate of the true contrast variable. In the following we will then apply a cut to keep timelines with a sufficient number of samples. Since the distributions are very broad we require at least $N_{int}(r) > 50$ contacts in a relation. We will study later the effect of this cut on the results. On the complete datasets, we are left with respectively 57, 26, 91 and 70 timelines for the *hosp*, *conf*, *malawi* and *baboons* datasets. We show the p.t.e distributions of the contact duration contrast for the 4 groups in Figure 4.

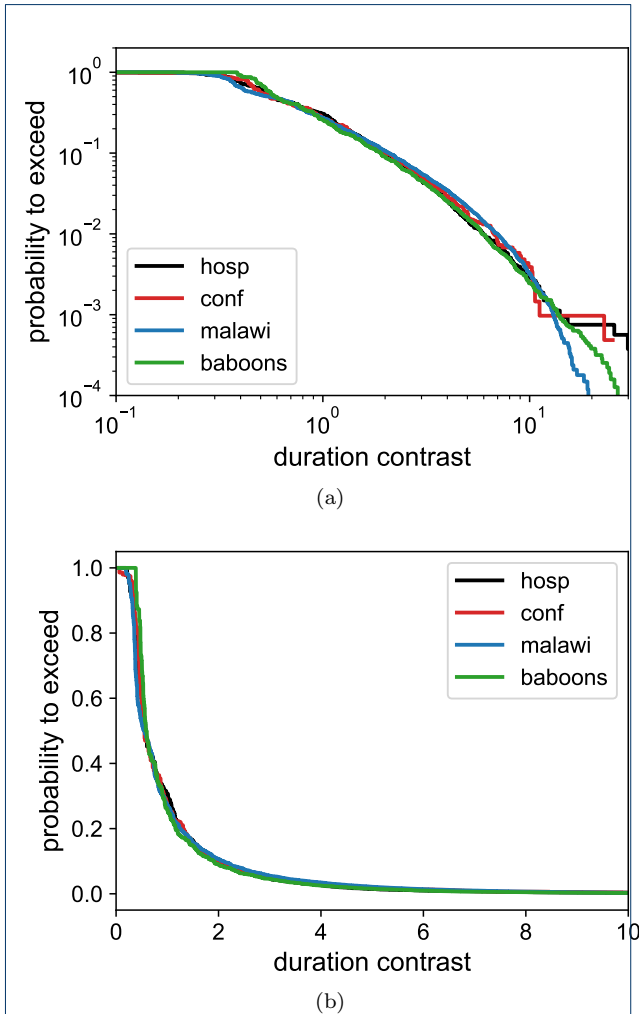


Figure 4 Distributions (p.t.e) of the duration contrast obtained for all relations within the same group satisfying $N_{int}(r) > 50$ in logarithmic (a) and linear scales (b). The complete datasets have been used (i.e. all days). The interaction mean-time corresponds to a value of 1. We then see for instance that the probability for an interaction to last longer than its mean-time is around 30%, but, rarely, it can exceed 10 times the mean-time.

The tails look now very similar up to 10 times the mean-time. The same distribution is observed on data from another conference, an office and a high-school (*SIAppendix*, *S2*). Thus, a (very) similar distribution is observed on 7 independent datasets.

To be more quantitative and assess the level of compatibility between the distributions, we use a Monte-Carlo method. For each dataset, we numerically invert the empirical distribution functions (which are one minus the p.t.e's shown on Figure 4) to construct the inverse cumulative function F^{-1} . We then draw N numbers u from a $[0, 1]$ uniform distribution, transform them with $F^{-1}(u)$ and reconstruct the p.t.e. The procedure is repeated 100 times and all distributions are plotted on top of each other on Figure 5.

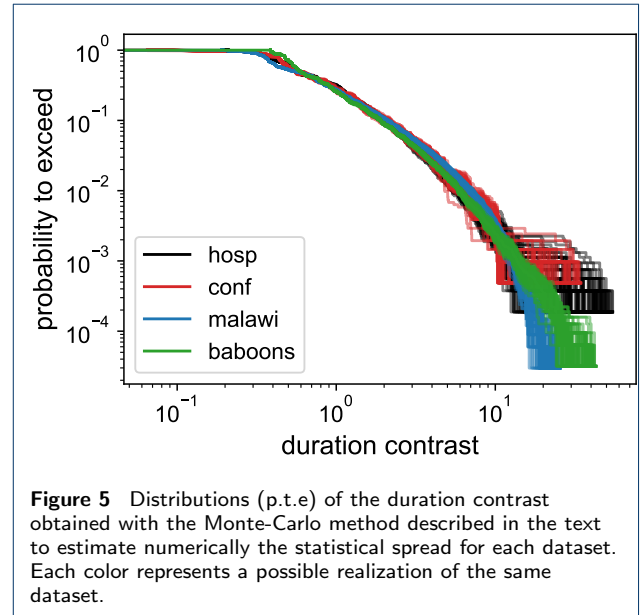


Figure 5 Distributions (p.t.e) of the duration contrast obtained with the Monte-Carlo method described in the text to estimate numerically the statistical spread for each dataset. Each color represents a possible realization of the same dataset.

One sees that the distributions are indeed all compatible in the $0.6 \lesssim \delta \lesssim 10$ range, where the upper bound comes from the limited sample size of the *hosp* and *conf* datasets, and the lower one from slight (but statistically significant) differences for low values. This will be our range of interest in the following.

Since the data-taking periods are very heterogeneous (ranging from 3 days for the *conf* and *hosp* datasets, to 12 and 26 for the *malawi* and *baboons* ones respectively) we have split the data day by day and verified that no particular one(s) particularly affects the results (*SIAppendix*, *S3-1*). We have also removed randomly a fraction of the agents (up to 50%), i.e. we removed all relations involving those agents, which did not affect the contrast distributions in a sizable way (*SIAppendix*, *S3-2*). Both tests confirm the robustness of the result.

Another option for studying deviations from the mean is to use the z -score

$$z_i(r) = \frac{t_i(r) - \bar{t}(r)}{\sigma(r)}, \quad (3)$$

where σ represents the standard-deviation of the duration values. The results obtained with this variable are very similar to the ones with the contrast (*SI Appendix, S4*) and we did not notice any difference on the tests that are presented later. Since the contrast variable is somewhat simpler (the z -score involving second order statistics) we only focus in the following on it.

We consider the impact of applying the $N_{int}(r) > 50$ cut. First, we note that similar results are obtained with a lower cut value as $N_{int} > 30$ (*SI Appendix, S5*). We then show that we can still reproduce the contrast distribution without any cut, using only the distributions with the cut (Figure 4). To this purpose we perform Monte-Carlo simulations. For a given dataset, for each relation (without any cut), we draw $N_{int}(r)$ random numbers following Figure 4 distribution to obtain $\delta_{i=1, \dots, N_{int}}$ contrast values. Those samples are obtained from the distribution with the $N_{int}(r) > 50$ cut, so with precise mean values that we call μ . We may mimic the statistical fluctuations due to any $N_{int}(r)$ value, by using the ratio

$$\delta_i^{mes} = \frac{\delta_i}{\frac{1}{N_{int}} \sum_i \delta_i} = \frac{t_i/\mu}{\frac{1}{N_{int}} \sum_i t_i/\mu} = \frac{t_i}{\bar{t}} \quad (4)$$

since μ actually cancels out. We compare the measured contrast distribution to the one observed on data, this time without any $N_{int}(r)$ cut, in Figure 6 for the *conf* dataset. We reproduce correctly the whole contrast distribution using only the Figure 4 one obtained with $\simeq 1\%$ of the data ($N_{int} > 50$). Similar results are obtained on the other datasets (*SI Appendix, S6.1*). This shows that the contrast distribution obtained from the large sample statistics is sufficient to reproduce any number of interactions, including small-sample ones. In other words, the $N_{int}(r) > 50$ cut only cleans the data without affecting the underlying “true” contrast distribution.

To check that the contrast distribution is not artificially produced by the procedure of dividing the timelines by their mean value, we use the *hosp* dataset to retrieve the set of interacting agents and their corresponding characteristics $N_{int}(r)$ and $\bar{t}(r)$. We then draw $N_{int}(r)$ random numbers following a Poisson distribution of parameter $\bar{t}(r)$ and recompute the contrast. The result is shown in Figure 7 which is clearly different from the results observed on the data.

The shape of the observed contrast distribution (Figure 4) is nontrivial. It is neither of exponential nor of

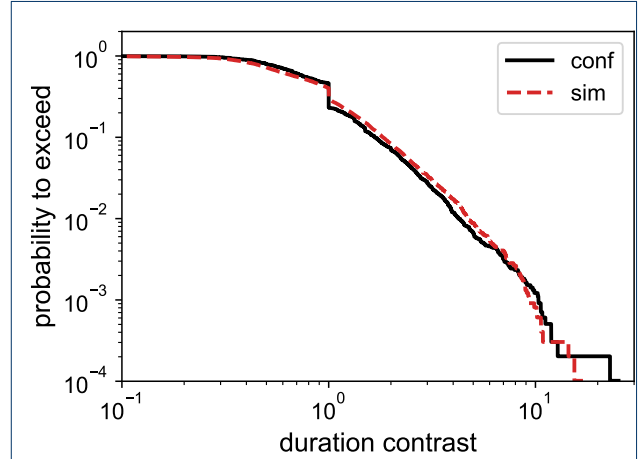


Figure 6 Distributions (p.t.e) of the duration contrast obtained for all relations in the *conf* dataset and simulations produced using the corresponding Figure 4 distribution (see text for details). The dip at 1 comes from numerous cases (65%) where $N_{int}=1$ always leads to $\delta = 1$.

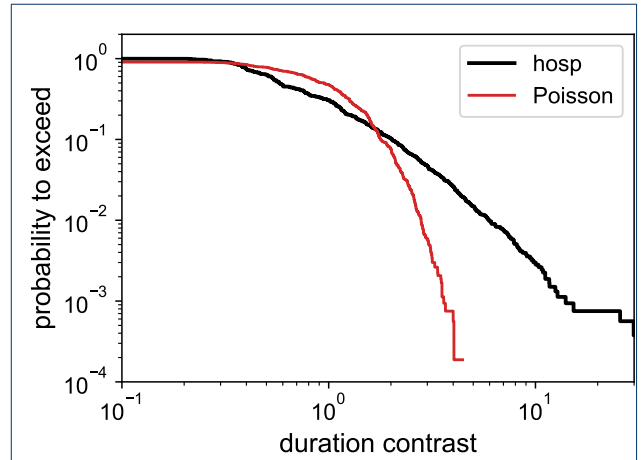


Figure 7 Distribution of the contrast duration assuming a Poisson distributed duration (in red). The parameters are taken from the *hosp* dataset. The result obtained in real data is shown in black.

power-law form. A stretched-exponential form is neither satisfactory. Empirically, we could obtain a reasonable fit in the $0.6 \lesssim \delta \lesssim 10$ region, by combining both a power-law and an exponential function

$$p(> \delta) = 0.3e^{-0.2\delta}/\delta^{1.1} \quad (5)$$

The denominator is here to enhance short contrasts, while the exponential term describes the long ones. This could be an indication of the existence of two regimes, one for short times when communications are more informative and a longer one when real conversations form [27]

At this point, we have shown that the *combined* contrast duration (i.e. for all relations) follows a very similar distribution. We now consider *each* relation separately and show in Figure 8 a superposition of the contrast duration distributions with the $N_{int}(r) > 50$ cut (similar results are observed without it but are, as expected, more noisy (see *SI Appendix, S6.2*).

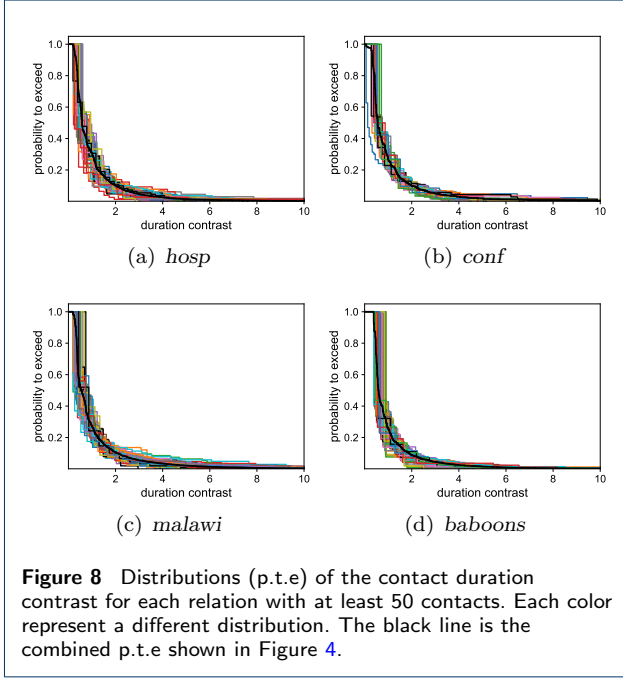


Figure 8 Distributions (p.t.e) of the contact duration contrast for each relation with at least 50 contacts. Each color represent a different distribution. The black line is the combined p.t.e shown in Figure 4.

They *all* follow rather closely the common contrast distribution. In other words, while the choice of individuals we meet (Figure 1), the interaction rate (Figure 3(a)) and mean-time spent together (Figure 3(b)) varies strongly with the environment, the propensity to spend more (or less) time than usual with a given individual, is remarkably similar. This points to the idea that once a face-to-face contact is triggered it follows its own dynamics, out of the sociological context.

For the sake of completeness, we note that we found no sizable correlations between the contact duration within the timelines (see *SI Appendix, S7*). This indicates one can draw independent samples using eq. (5).

We also considered the inter-contact (or “gap”) time in the relations to see whether its contrast reveals features similar to the duration ones. This is not the case as shown in Figure 9. The contrast of the inter-contact time thus seems to be more dependent on the sociological context.

3 Comparison with a model

The contrast distribution can be used as a new metric when studying face-to-face temporal graphs in order to test and improve existing agent-based models designed

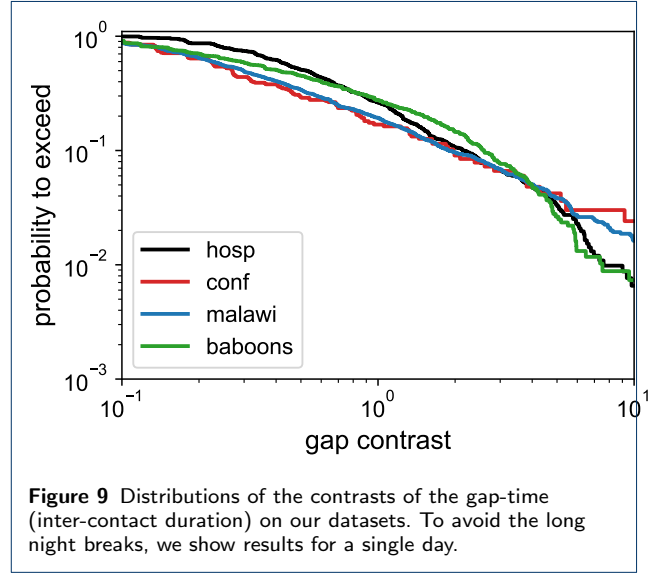


Figure 9 Distributions of the contrasts of the gap-time (inter-contact duration) on our datasets. To avoid the long night breaks, we show results for a single day.

to reproduce the full evolution of a set of individuals. For instance, the “force directed motion” (FDM) model is successful in describing several key features of observed face-to-face interactions [6]. Based on the idea of attractiveness between some agents performing a random-walk within a bounded perimeter [4, 28], the model further includes the concept of “similarity” between two individuals [29], known as homophily in social sciences. The similarity s_{ij} influences the time two agents spend together and the way the random-walk is biased. The model assumes that the contact duration between two agents is exponentially distributed with a rate s_{ij}/μ_1 , where μ_1 is adjusted on the data to reproduce the overall duration of contacts. We have run the code provided by the authors with their setup corresponding to the *hosp* dataset, to test the distribution of the contrast variable. Figure 10 shows that the model distribution falls too steeply. We have tried adapting the parameters and some parts of the code but could not find a configuration giving a better contrast distribution (see *SI Appendix, S8*) [2].

Modeling correctly the tails of the contact duration is also essential in epidemiological studies since the spread of a disease happens mostly during long interactions. For a given mean-interaction time, eq. (5) allows to simulate a much more realistic duration of contacts than a Poissonian one. This can be used in SIR-like statistical inference, or using agent-based models, for the precise modeling of long interactions.

^[2]The authors of [6] also quote some results obtained with a hyperbolic geometry [30] but, due to the lack of public software, we could not test it

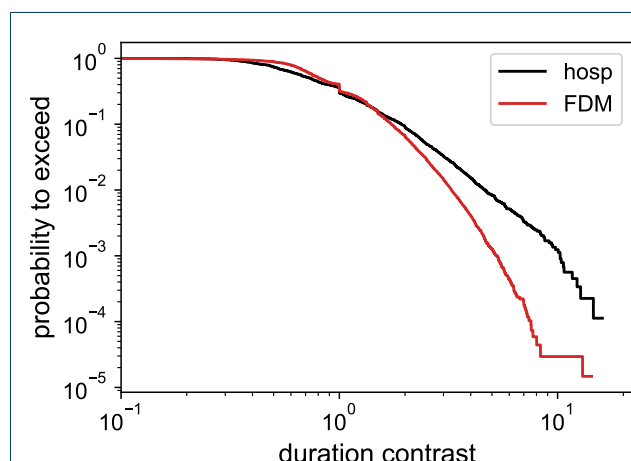


Figure 10 Comparison of the contrast distributions obtained with the *hosp* dataset to the result of the “force-directed motion” (FDM) model [6]. We used the parameters provided by the authors and their dataset (slightly different from ours, due to a different selection). The FDM curve is the combined result from 10 simulations.

Conclusion

We have compared face-to-face interaction data taken in some very different environments; some were recorded in a European hospital and during a scientific conference, others in a small village in Africa. With the original intention to pinpoint differences with the results concerning humans, we have also included data on baboons’ interactions in an enclosure.

Although the topological structures (who interacts with whom) and the mean-time spent together are clearly dependent on the sociological environment, it appears that the deviations from the mean-time for each pair (do we spend more/less time than usual with a given person) follow a very similar distribution, including for baboons. We (and baboons) tend to interact most often for much less time than “usual” with a given individual and sometimes, but rarely, much longer. What is striking is that the distribution for this quantity, which we call the “relation contrast” looks universal. It is the same for people at a scientific conference or farmers in a small Malawi village (and baboons in an enclosure), see Figure 4 (also *SI Appendix, S2* for the 7 datasets).

These results suggests that, once a face-to-face contact is triggered, it follows its own dynamics independently from the social context. This is maybe not a big surprise to a sociologist in particular working in the field of Conversation Analysis [27] where it is postulated that each conversation follows some rules inde-

pendently from the social context [3]. But to our knowledge, this was not noticed by physicists and may help disentangling the topological and temporal aspects of face-to-face interactions.

The possible universality of the relation contrast must be challenged with more data. On the animal side, one should consider groups of animals with strong social interactions, that can be identified (labeled) and followed individually. Hominids, as baboons, are known to have social behaviors close to ours, which probably explains the similarity of the contrast distribution with the human’s one. Chimpanzee or bonobo’s data should show similar characteristic. Concerning mammals, we could think of tracking individuals in elephant herds or wolf packs but it’s difficult to acquire precise data in the wild. The most promising approach concerns the study of social insect networks [31]. Details about ant interactions is probably the most feasible since recent techniques allow to tag and follow each individual separately [32]. On the human side, we need to check whether the contrast is influenced by age. Since children perceive time differently from adults, following the contact patterns of young children in a nursery could provide a valuable insight into this question.

Availability of data and materials

- The datasets analyzed during the current study are available in the *sociopatterns* repository, www.sociopatterns.org
- The FDM code was downloaded on 10 June 2023 from https://bitbucket.org/mrodflr/similarity_forces
- The python3 software used to produce the results is available from <https://gitlab.in2p3.fr/plaszczyn/coll>
- The graph-related computations and Figure 1 were obtained with the graph-tool (v 2.43) software [33].

Author details

¹Université Paris-Saclay, CNRS/IN2P3, IJCLab, 91405, Orsay, France.

²Université Paris-Cité, IJCLab, 91405, Orsay, France. ³Center for Interdisciplinary Research in Biology (CIRB), Collège de France, CNRS, INSERM, Université PSL, Paris, France.

References

1. Song, C., Koren, T., Wang, P., Barabási, A.-L.: Modelling the scaling properties of human mobility. *Nature Physics* **6**(10), 818–823 (2010). doi:[10.1038/nphys1760](https://doi.org/10.1038/nphys1760)
2. Stehle, J., Barrat, A., Bianconi, G.: Dynamical and bursty interactions in social networks. *Physical Review E* **81**(3), 035101 (2010). doi:[10.1103/PhysRevE.81.035101](https://doi.org/10.1103/PhysRevE.81.035101). [1002.4109](https://doi.org/10.1002.4109)
3. Zhao, K., Stehle, J., Bianconi, G., Barrat, A.: Social network dynamics of face-to-face interactions. *Physical Review E* **83**(5), 056109 (2011). doi:[10.1103/PhysRevE.83.056109](https://doi.org/10.1103/PhysRevE.83.056109). [1102.2423](https://doi.org/10.1002.2423)
4. Starnini, M., Baronchelli, A., Pastor-Satorras, R.: Modeling Human Dynamics of Face-to-Face Interaction Networks. *Physical Review Letters* **110**(16), 168701 (2013). doi:[10.1103/PhysRevLett.110.168701](https://doi.org/10.1103/PhysRevLett.110.168701)
5. Sekara, V., Stopczynski, A., Lehmann, S.: Fundamental structures of dynamic social networks. *Proceedings of the National Academy of Sciences* **113**(36), 9977–9982 (2016). doi:[10.1073/pnas.1602803113](https://doi.org/10.1073/pnas.1602803113). [1506.04704](https://doi.org/10.1506.04704)

[3] The fact that similar results are observed on baboons requires however to enlarge the concept of “discussion”.

6. Flores, M.A.R., Papadopoulos, F.: Similarity Forces and Recurrent Components in Human Face-to-Face Interaction Networks. *Physical Review Letters* **121**(25), 258301 (2018). doi:[10.1103/PhysRevLett.121.258301](https://doi.org/10.1103/PhysRevLett.121.258301)
7. Barbosa, H., Barthelemy, M., Ghoshal, G., James, C.R., Lenormand, M., Louail, T., Menezes, R., Ramasco, J.J., Simini, F., Tomasini, M.: Human mobility: Models and applications. *Physics Reports* **734**, 1–74 (2018). doi:[10.1016/j.physrep.2018.01.001](https://doi.org/10.1016/j.physrep.2018.01.001)
8. Hui, P., Chaintreau, A., Scott, J., Gass, R., Crowcroft, J., Diot, C.: Pocket switched networks and human mobility in conference environments. In: *Proceeding of the 2005 ACM SIGCOMM Workshop on Delay-tolerant Networking - WDTN '05*, pp. 244–251. ACM Press, Philadelphia, Pennsylvania, USA (2005). doi:[10.1145/1080139.1080142](https://doi.org/10.1145/1080139.1080142)
9. Scherrer, A., Borgnat, P., Fleury, E., Guillaume, J.-L., Robardet, C.: Description and simulation of dynamic mobility networks. *Computer Networks* **52**(15), 2842–2858 (2008). doi:[10.1016/j.comnet.2008.06.007](https://doi.org/10.1016/j.comnet.2008.06.007). Accessed 2022-09-03
10. Cattuto, C., Van den Broeck, W., Barrat, A., Colizza, V., Pinton, J.-F., Vespignani, A.: Dynamics of Person-to-Person Interactions from Distributed RFID Sensor Networks. *PLoS ONE* **5**(7), 11596 (2010). doi:[10.1371/journal.pone.0011596](https://doi.org/10.1371/journal.pone.0011596)
11. Barrat, A., Cattuto, C., Tozzi, A.E., Vanhems, P., Voirin, N.: Measuring contact patterns with wearable sensors: Methods, data characteristics and applications to data-driven simulations of infectious diseases. *Clinical Microbiology and Infection* **20**(1), 10–16 (2014). doi:[10.1111/1469-0691.12472](https://doi.org/10.1111/1469-0691.12472)
12. Stehlé, J., Voirin, N., Barrat, A., Cattuto, C., Colizza, V., Isella, L., Régis, C., Pinton, J.-F., Khanafer, N., Van den Broeck, W., Vanhems, P.: Simulation of an SEIR infectious disease model on the dynamic contact network of conference attendees. *BMC Medicine* **9**(1), 87 (2011). doi:[10.1186/1741-7015-9-87](https://doi.org/10.1186/1741-7015-9-87)
13. Isella, L., Stehlé, J., Barrat, A., Cattuto, C., Pinton, J.-F., Van den Broeck, W.: What's in a crowd? Analysis of face-to-face behavioral networks. *Journal of Theoretical Biology* **271**(1), 166–180 (2010). doi:[10.1016/j.jtbi.2010.11.033](https://doi.org/10.1016/j.jtbi.2010.11.033)
14. Starnini, M., Baronchelli, A., Barrat, A., Pastor-Satorras, R.: Random walks on temporal networks. *Physical Review E* **85**(5), 056115 (2012). doi:[10.1103/PhysRevE.85.056115](https://doi.org/10.1103/PhysRevE.85.056115)
15. Génois, M., Vestergaard, C.L., Fournet, J., Panisson, A., Bonmarin, I., Barrat, A.: Data on face-to-face contacts in an office building suggest a low-cost vaccination strategy based on community linkers. *Network Science* **3**(3), 326–347 (2015). doi:[10.1017/nws.2015.10](https://doi.org/10.1017/nws.2015.10)
16. Vanhems, P., Barrat, A., Cattuto, C., Pinton, J.-F., Khanafer, N., Régis, C., Kim, B.-a., Comte, B., Voirin, N.: Estimating Potential Infection Transmission Routes in Hospital Wards Using Wearable Proximity Sensors. *PLoS ONE* **8**(9), 73970 (2013). doi:[10.1371/journal.pone.0073970](https://doi.org/10.1371/journal.pone.0073970)
17. Fournet, J., Barrat, A.: Contact Patterns among High School Students. *PLoS ONE* **9**(9), 107878 (2014). doi:[10.1371/journal.pone.0107878](https://doi.org/10.1371/journal.pone.0107878)
18. Mastrandrea, R., Fournet, J., Barrat, A.: Contact patterns in a high school: A comparison between data collected using wearable sensors, contact diaries and friendship surveys. *PLoS ONE* **10**(9), 0136497 (2015). doi:[10.1371/journal.pone.0136497](https://doi.org/10.1371/journal.pone.0136497)
19. Kiti, M.C., Tizzoni, M., Kinyanjui, T.M., Koech, D.C., Munywoki, P.K., Meriac, M., Cappa, L., Panisson, A., Barrat, A., Cattuto, C., Nokes, D.J.: Quantifying social contacts in a household setting of rural Kenya using wearable proximity sensors. *EPJ Data Science* **5**(1), 21 (2016). doi:[10.1140/epjds/s13688-016-0084-2](https://doi.org/10.1140/epjds/s13688-016-0084-2)
20. Ozella, L., Paolotti, D., Lichand, G., Rodríguez, J.P., Haenni, S., Phuka, J., Leal-Neto, O.B., Cattuto, C.: Using wearable proximity sensors to characterize social contact patterns in a village of rural Malawi. *EPJ Data Science* **10**(1), 46 (2021). doi:[10.1140/epjds/s13688-021-00302-w](https://doi.org/10.1140/epjds/s13688-021-00302-w)
21. Gelardi, V., Godard, J., Paleressompoulle, D., Claidiere, N., Barrat, A.: Measuring social networks in primates: wearable sensors versus direct observations. *Proceedings of the Royal Society A: Mathematical, Physical and Engineering Sciences* **476**(2236), 20190737 (2020). doi:[10.1098/rspa.2019.0737](https://doi.org/10.1098/rspa.2019.0737)
22. Barrat, A., Cattuto, C.: Face-to-Face Interactions. In: Gonçalves, B., Perra, N. (eds.) *Social Phenomena*, pp. 37–57. Springer International Publishing, Cham (2015). doi:[10.1007/978-3-319-14011-7_3](https://doi.org/10.1007/978-3-319-14011-7_3)
23. Génois, M., Barrat, A.: Can co-location be used as a proxy for face-to-face contacts? *EPJ Data Science* **7**(1), 11 (2018). doi:[10.1140/epjds/s13688-018-0140-1](https://doi.org/10.1140/epjds/s13688-018-0140-1)
24. Newman, M.E.J.: Power laws, Pareto distributions and Zipf's law. *Contemporary Physics* **46**(5), 323–351 (2005). doi:[10.1080/00107510500052444](https://doi.org/10.1080/00107510500052444). [cond-mat/0412004](https://doi.org/10.1080/00107510500052444)
25. Barrat, A., Barthélemy, M., Pastor-Satorras, R., Vespignani, A.: The architecture of complex weighted networks. *Proceedings of the National Academy of Sciences* **101**(11), 3747–3752 (2004). doi:[10.1073/pnas.0400087101](https://doi.org/10.1073/pnas.0400087101)
26. Peebles, P.J.E.: III.62. The large-scale structure of the universe. Princeton University Press, ??? (1980)
27. Button, G., Lynch, M., Sharrock, W.: *Ethnomethodology, Conversation Analysis and Constructive Analysis: On Formal Structures of Practical Action*, 1st edn. Routledge, London (2022). doi:[10.4324/9781003220794](https://doi.org/10.4324/9781003220794)
28. Starnini, M., Baronchelli, A., Pastor-Satorras, R.: Model reproduces individual, group and collective dynamics of human contact networks. *Social Networks* **47**, 130–137 (2016). doi:[10.1016/j.socnet.2016.06.002](https://doi.org/10.1016/j.socnet.2016.06.002)
29. Papadopoulos, F., Kitsak, M., Serrano, M.Á., Boguñá, M., Krioukov, D.: Popularity versus similarity in growing networks. *Nature* **489**(7417), 537–540 (2012). doi:[10.1038/nature11459](https://doi.org/10.1038/nature11459)
30. Krioukov, D., Papadopoulos, F., Kitsak, M., Vahdat, A., Boguñá, M.: Hyperbolic geometry of complex networks. *Physical Review E* **82**(3), 036106 (2010). doi:[10.1103/PhysRevE.82.036106](https://doi.org/10.1103/PhysRevE.82.036106)
31. Fewell, J.H.: Social Insect Networks. *Science* **301**(5641), 1867–1870 (2003). doi:[10.1126/science.1088945](https://doi.org/10.1126/science.1088945)
32. Greenwald, E., Segre, E., Feinerman, O.: Ant trophallactic networks: Simultaneous measurement of interaction patterns and food dissemination. *Scientific Reports* **5**(1), 12496 (2015). doi:[10.1038/srep12496](https://doi.org/10.1038/srep12496)
33. Peixoto, T.P.: The graph-tool python library. figshare (2014). doi:[10.6084/m9.figshare.1164194](https://doi.org/10.6084/m9.figshare.1164194). Accessed 2014-09-10

On the duration of face-to-face contacts

Supplementary Information

S. Plaszczynski, G. Nakamura, B. Grammaticos, and M. Badoual

February 7, 2024

Contents

S1 Main result	2
S2 Other datasets	2
S3 On the robustness of the results	3
S3.1 Day by day variation	3
S3.2 Varying the network size (and topology)	4
S4 z-scores	5
S5 Number of interactions	6
S6 Simulations without a minimal number of interactions	6
S6.1 Combined contrast	6
S6.2 Contrast per relation	6
S7 Contact duration correlations	10
S8 FDM model	10

S1 Main result

Our main result concerns the duration of face-to-face contacts between *each* pair of individuals. Although the mean-interaction time varies, the *deviation* from this mean value is very similar in several very different social contexts. As in other fields of physics (e.g cosmology) we call this over/under-duration the duration *contrast*. It is a dimensionless value that describes how much given an interaction is longer or shorter than its usual (mean) time and can be expressed in percents. By construction its mean value is 1.

To remove some statistical noise, we only use data where there is a sufficient number of interactions (samples) N_{int} . Since the duration distribution is heavy-tailed we use a large minimal value of 50.

Figure 1 (a) shows how the distribution of the duration of contacts and how it changes when computing the contrast in (b). Both use the $N_{int} > 50$ cut.

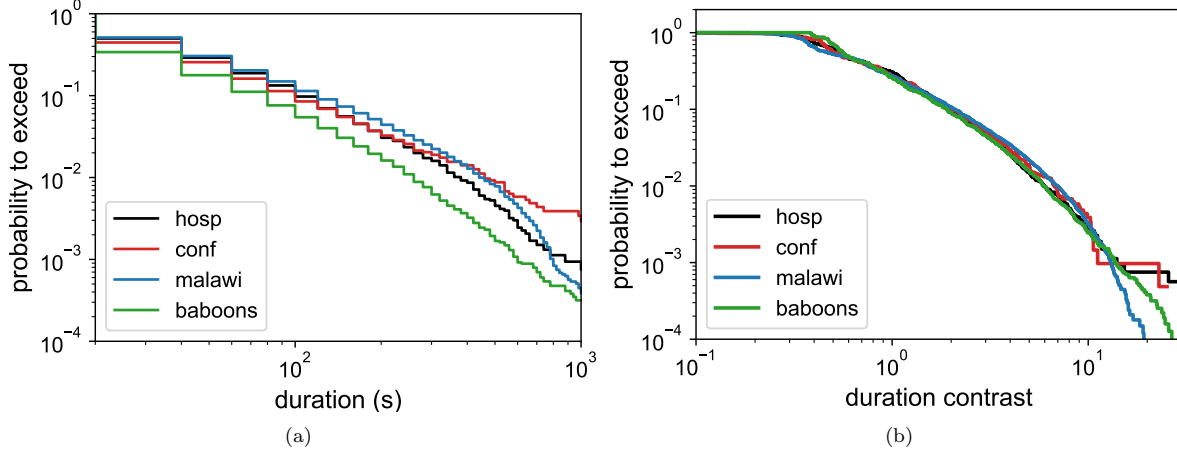


Figure 1: (a) distributions (p.t.e) of the duration of contact and (b) contrast duration on the 4 datasets. The cut $N_{int} > 50$ is used for both.

S2 Other datasets

Although in our work we have focused on sociologically most dissimilar datasets, we have also looked at some other data provided by the *sociopattern* collaboration.

1. *conf2*: these are data taken at another conference (SFHH,[1, 2]) with $\simeq 380$ participants for 2 days.
2. *office*: data taken at an office (Intitut de Veille Sanitaire near Paris, [3, 4]) with about 165 participants for 10 days.
3. *highschool*: data from a french high-school, near Marseille [5, 6]. About 300 participants for 4 days

As in Sect. S1 we show how using the contrast standardizes the contact duration on Figure 2 on these new datasets; for comparison we also included the previous *conf* result and still use the $N_{int} > 50$ cut.

The contrast distributions are similar to the results presented in the paper, and differences are barely noticeable in a linear representation.

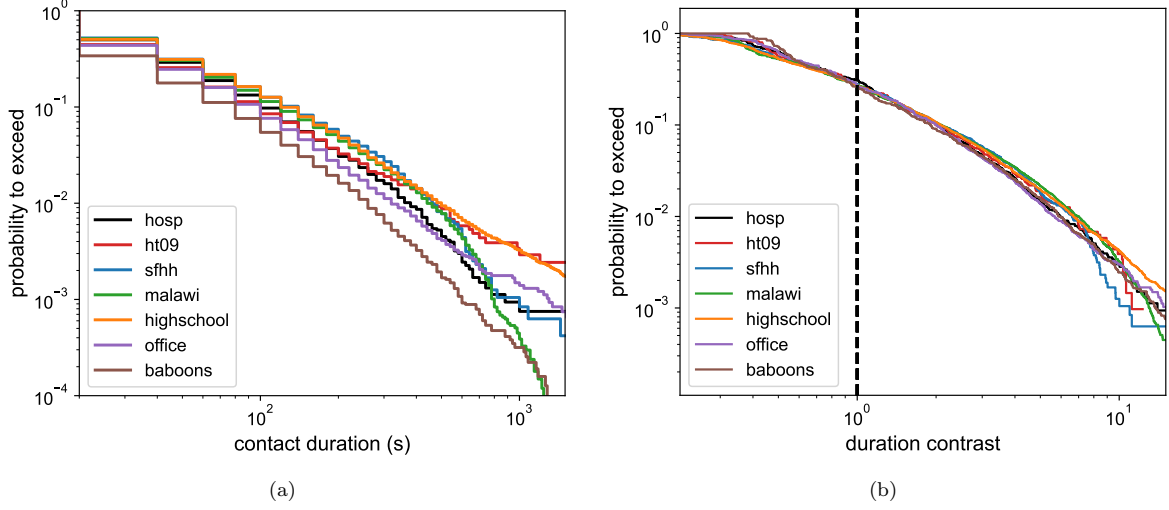


Figure 2: (a) distributions (p.t.e) of the duration of contact and (b) contrast duration for 3 other datasets.

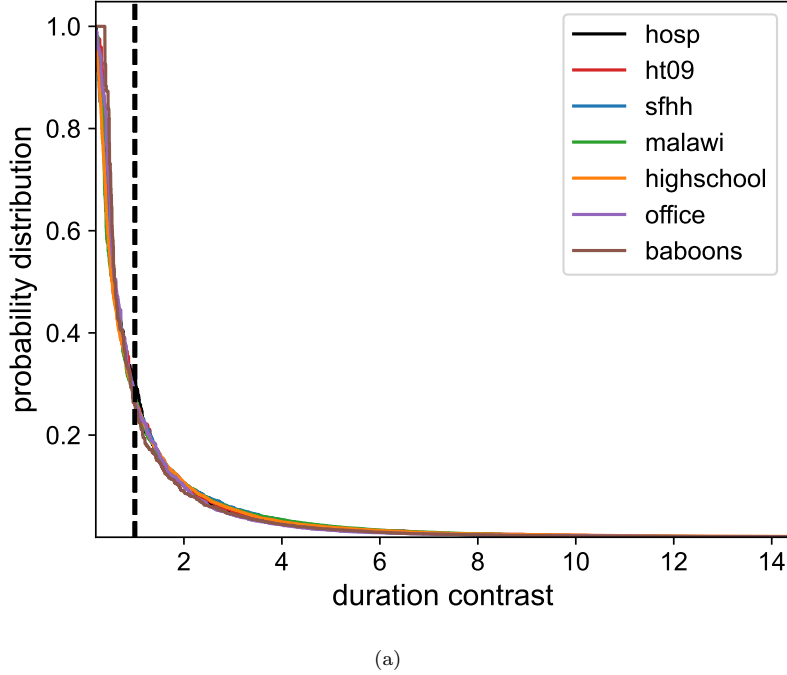


Figure 3: Same as Figure 2 (b) in linear scale.

S3 On the robustness of the results

S3.1 Day by day variation

The datasets are very heterogeneous in size as shown in the paper Table 1. The *malawi* and *baboons* ones have more data-taking days (12 and 26). Increasing the data size actually affects essentially the very end of the p.t.e tail as shown on the paper Fig.5, since it probes very rare events. To check that a single day does not bias the results for the lengthy datasets, we have split the data day by day and the results are presented on Figure 4.

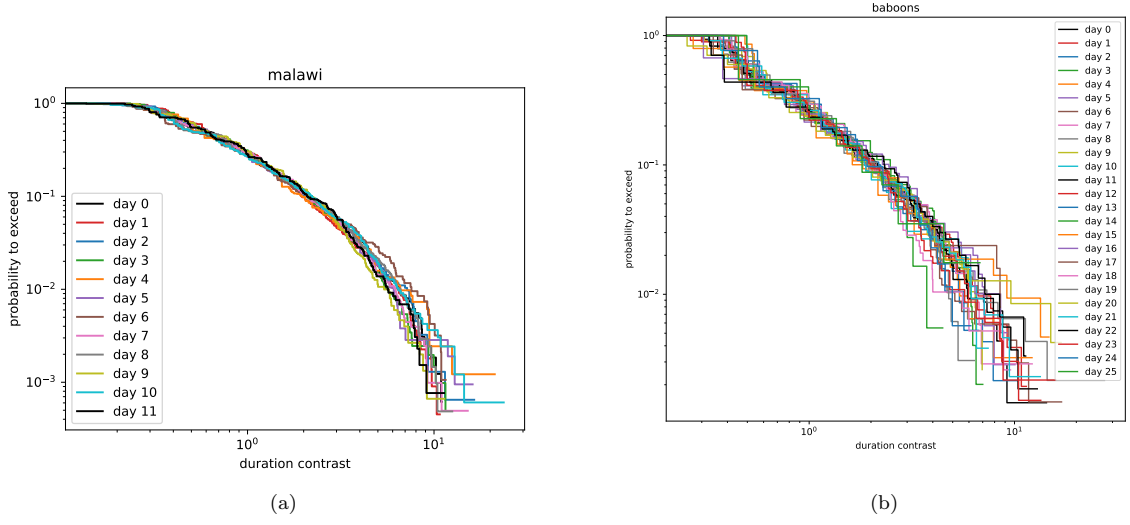


Figure 4: Distributions (p.t.e) of the duration contrast for the *malawi* (a) and *baboons* (b) datasets splitting the samples day by day.

S3.2 Varying the network size (and topology)

The number of agents (then size of the graphs) varies among the datasets (see Table 1). As shown on Fig 1., the topologies are also very different. If there is a common process different sizes and topologies of the network were thus tested.

To test whether a particular set of individuals could influence the shape of the contrast distributions we have further performed the following test: we removed some fraction of random individuals from the full list of relations. The distributions obtained when removing (randomly) 50% of individuals on the *malawi* dataset are shown on Figure 5 (similar results are obtained with the other datasets).

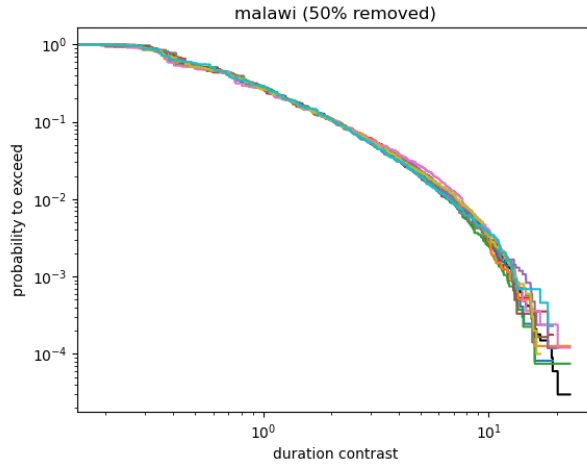


Figure 5: Distributions (p.t.e) of the duration contrast for the *malawi* datasets after removing 50% of the agents. Different colors represent different random realizations of the removed agents.

It shows that the distributions are very robust to the size of the network (and thus its topology) and not driven by a particular set of vertices.

S4 z-scores

We have characterized deviations from mean-values by the contrast variable which is simply obtained by rescaling the sample values by the mean. Another dimensionless quantity that can be build to probe deviations from mean values is the z-score

$$z_i(r) = \frac{t_i(r) - \bar{t}(r)}{\sigma(r)}, \quad (1)$$

where σ represents the standard-deviation of the values.

Here t_i is the contact duration or the gap time. We show the p.t.e distributions for both quantities on Figure 6.

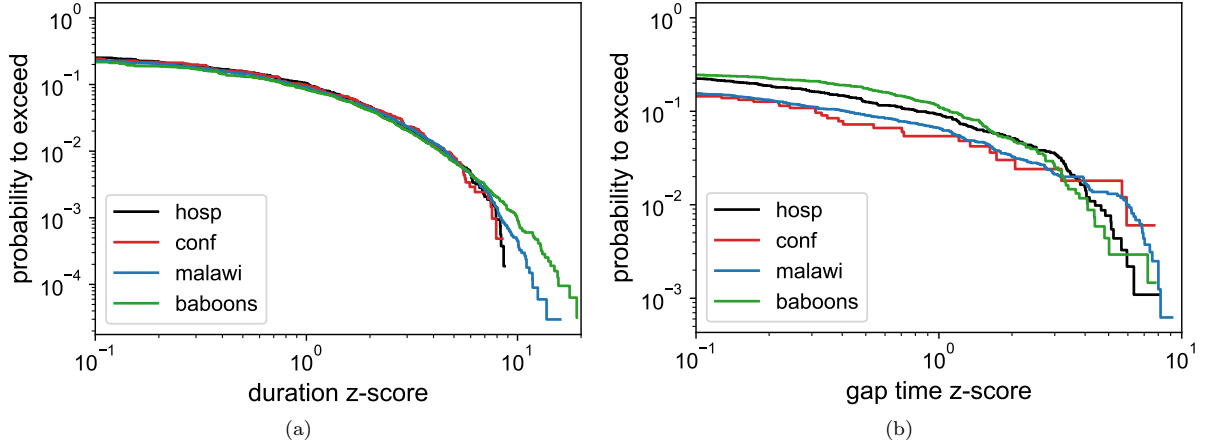


Figure 6: (a) Distributions (p.t.e) of z-scores for the duration (b) and gap-time. Note that the values can become negative and cannot be shown on such logarithmic plots (which is why distributions do not start at 1).

The distributions show a behavior that is similar to the one obtained using the contrast variable. They may even seem more regular at small z-scores, but this is an artifact due to using a logarithmic axis. Indeed z-scores can become negative (while the contrast cannot). Representing it for the duration with a linear scale one obtains Figure 7. There are some differences around -0.5 which are the counterpart of what is observed near 0.4 on the contrast plot (Figure 1 (b)).

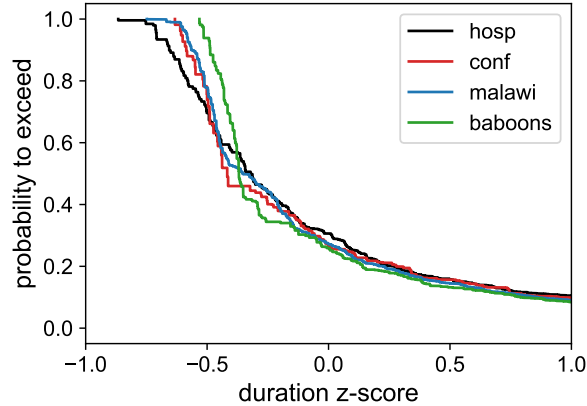


Figure 7: Zoom of Figure 6 on the negative part of the distribution using a linear axis.

Using the z-score thus does not change our conclusion on the gap-time which looks more context-dependent. Overall the results obtained with z-scores are very consistent with the ones obtained with the contrast on which we focus in the paper.

S5 Number of interactions

To compute a mean value one traditionally invokes the central limit theorem and compute a reliable arithmetic mean with $\simeq 20$ samples . However the contact duration distribution is very wide (Figure 1(a)) so we prefer to increase that value to $N_{int} > 50$ before computing the contrast, still keeping a reasonable number of timelines in each case. We may use a lower cutoff and the contrasts distributions are still similar(Figure 8) . But we have added some noisy samples. Note that this value of 50 is only dictated by the data limit data-taking period. Had we a really long period, the mean interaction times between each pair would be well known and this cut would be not necessary.

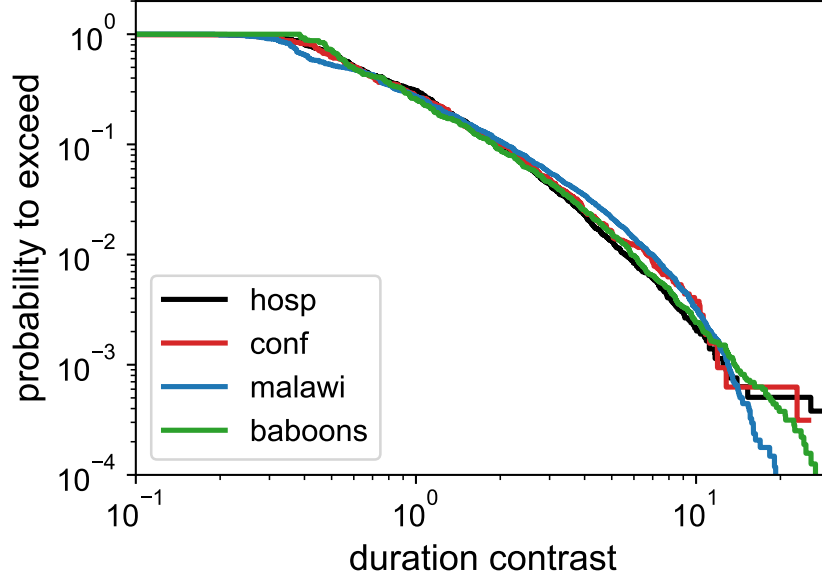


Figure 8: Distribution of the contrast duration on the 4 datasets using a $N_{int}(r) > 30$ cut.

S6 Simulations without a minimal number of interactions

S6.1 Combined contrast

We have shown in the manuscript how to reproduce the noise present on the data for all N_{int} values on the *conf* dataset in Section 3. Figure 9 shows the results for the other datasets. We reproduce all the data, using only a small fraction of the timelines (the ones with $N_{int} > 50$ which represents respectively).

S6.2 Contrast per relation

In the previous section, the duration (and contrast) of all contacts are combined on Figure 9 in the sense the contrast of each relation are mixed together. We now consider each relation and show its contrast p.t.e with different colors. The timelines are noisy since we do not use any minimal number of steps (N_{int}). The *baboons* result is less noisy but this is only due to the fact that the timelines have more samples due to the longer data-taking period (26 days).

We then perform the same simulations than described in the manuscript, but this time on each relation individually. Once again only the global shape of the contrast obtained with the $N_{int} > 50$ cut (i.e. Figure 1(b)) is used to draw the random numbers. The results are shown on Figure 11. They resembles closely the data (Figure 10). This confirms that the shape and spread observed on data (Figure 10) can be reproduced using only the cleaned Figure 1 distribution ($N_{int}(r) > 50$ and statistical fluctuations (on the mean) due to the limited size statistics.

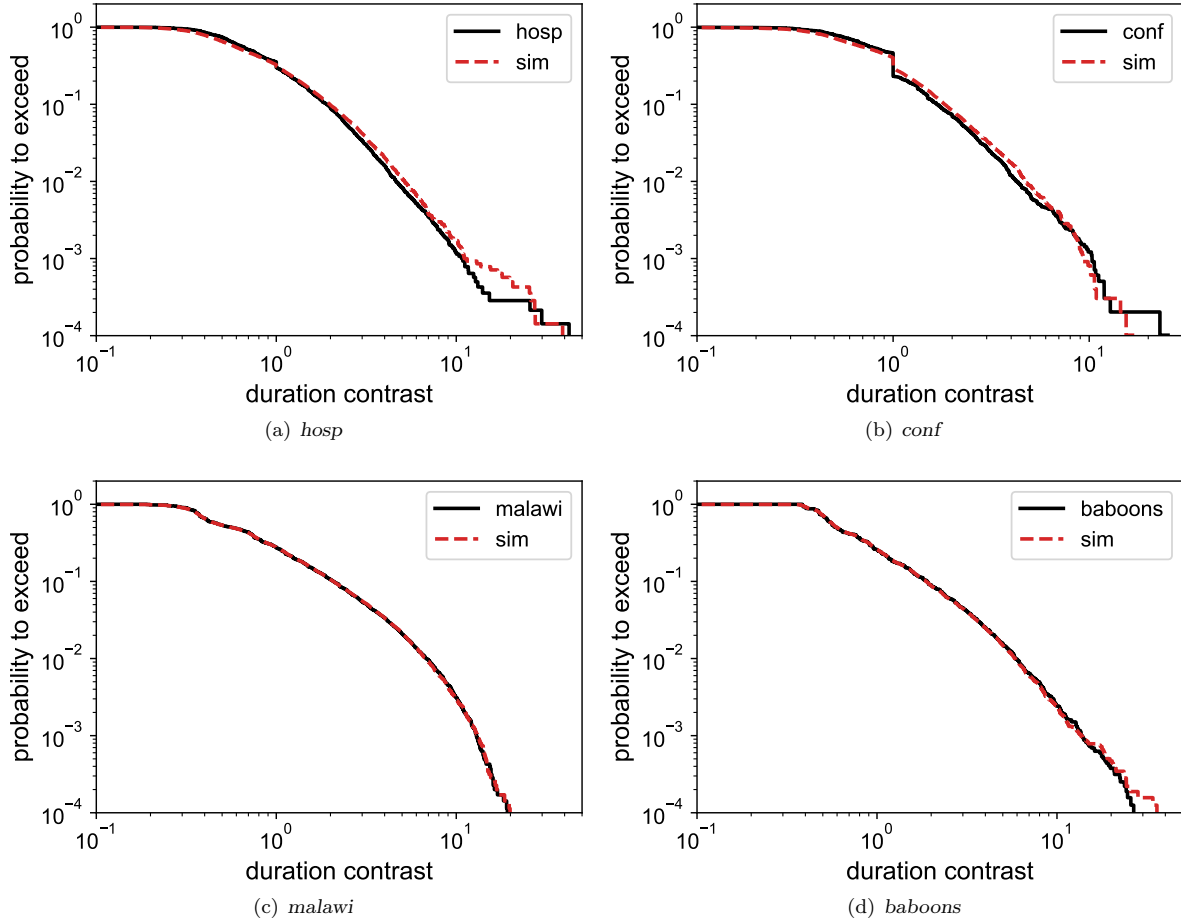


Figure 9: Results of the simulations described in the manuscript (Sect 3) without using a cut on N_{int} for all the datasets.

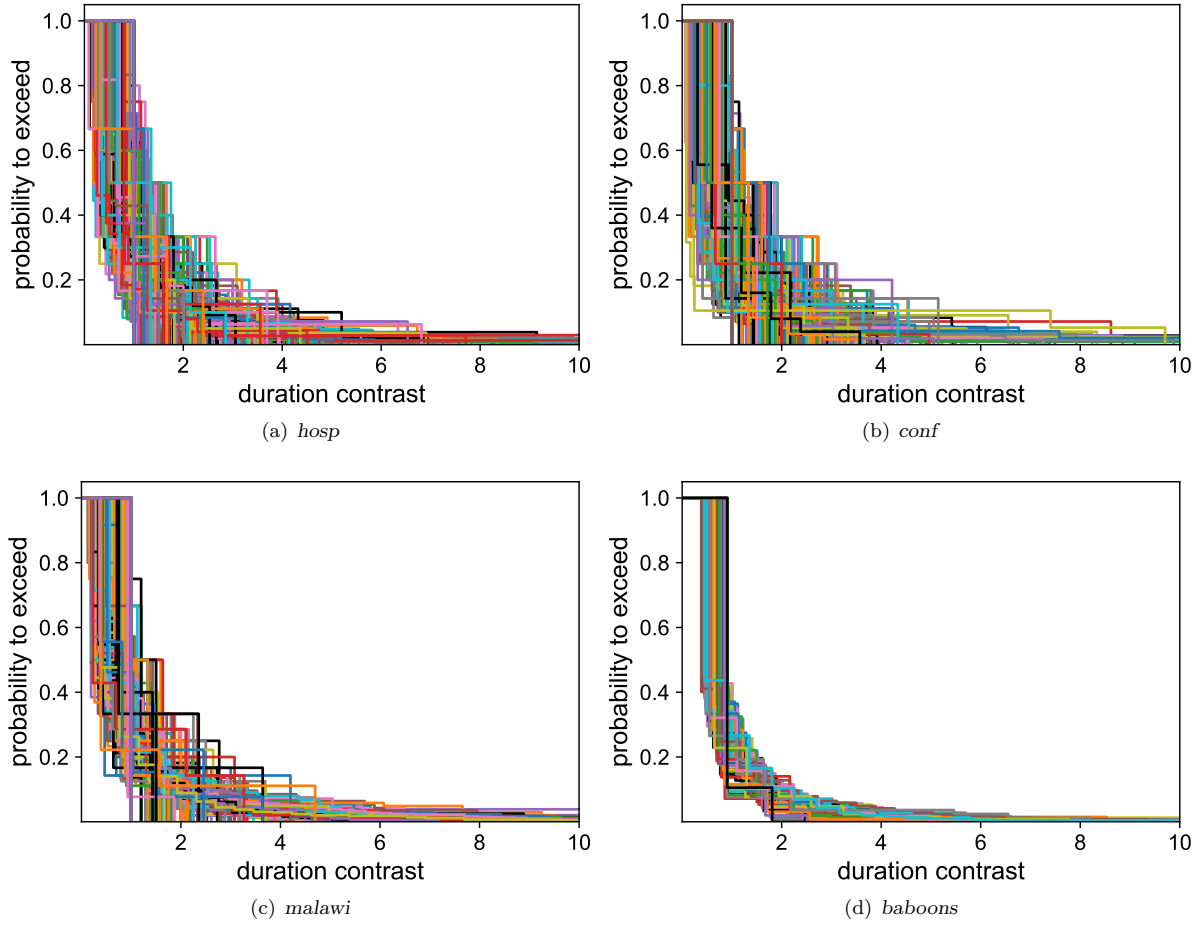


Figure 10: Contrast distributions per relation measured on the data without any N_{int} cut. Each color represents a different relation timeline.

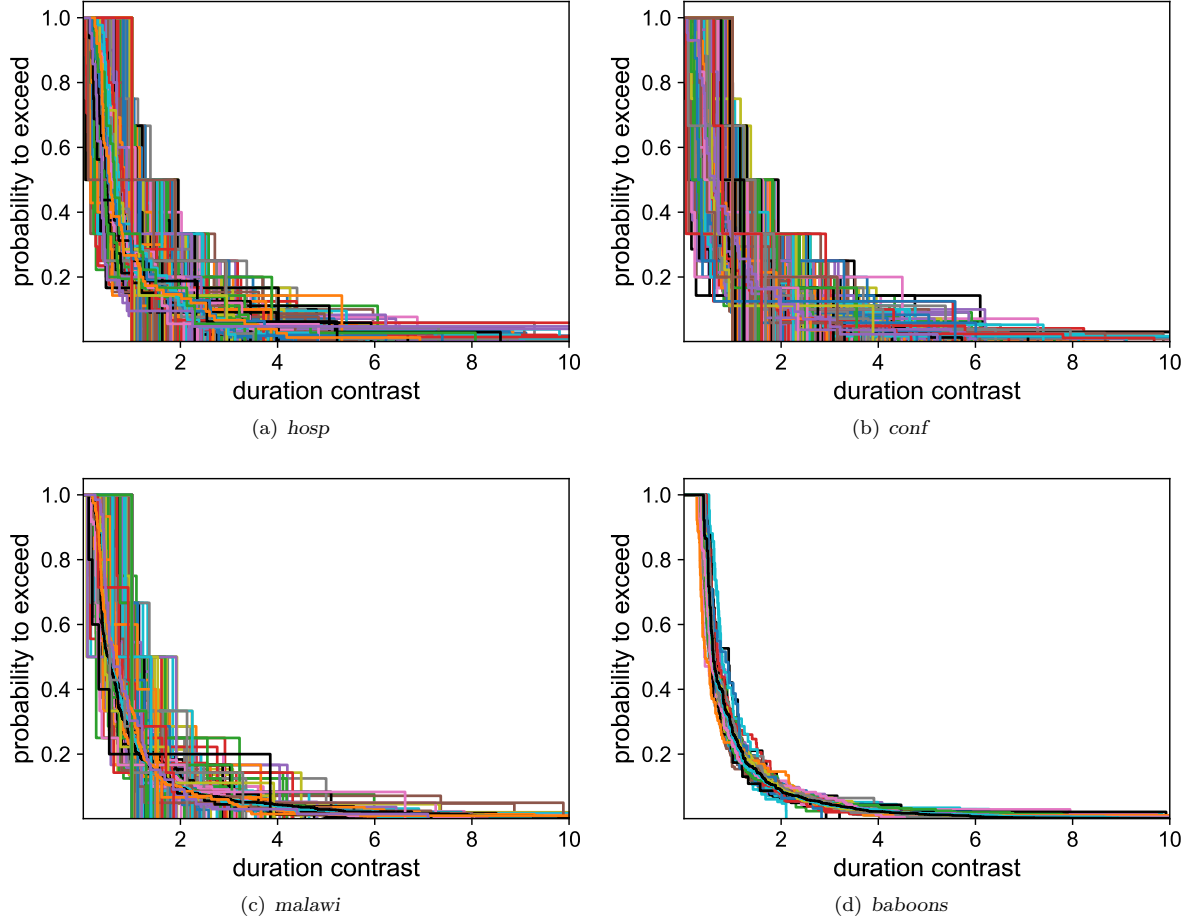


Figure 11: Results of the simulations described in the manuscript (Sect 3) for each relation (colored curves) without using a cut on N_{int} for all the datasets.

S7 Contact duration correlations

To test if some temporal correlations appear in the timelines, we compute the power-spectral density for each relation with the classical Welch periodogram method. Figure 12 obtained with the *malawi* data shows the result.

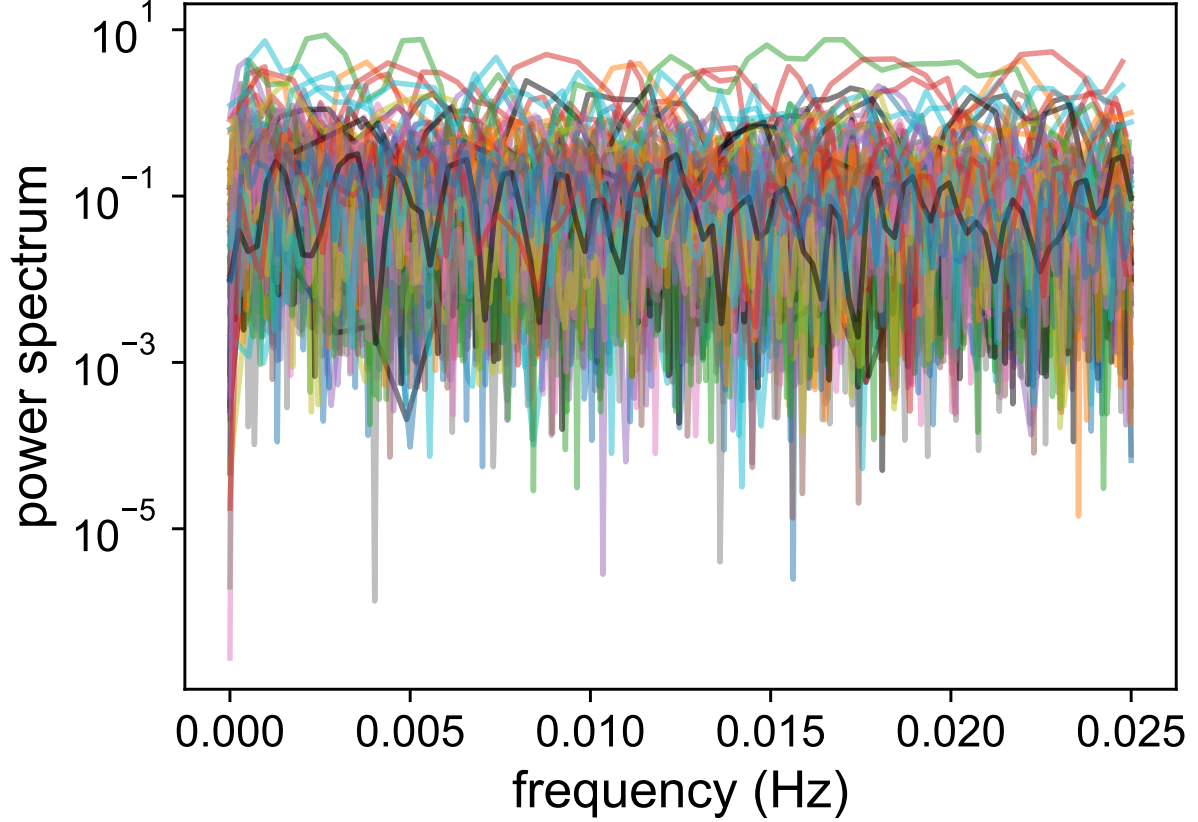


Figure 12: Power-spectra density measured

The spectra are essentially flat indicating no sizable temporal correlations within the timelines.

S8 FDM model

The FDM model has in its base configuration 4 free parameters that were adjusted by the authors of [7] to reproduce several key aspects of the evolving temporal graph of relations. The parameters are

1. μ_1 which impacts the contact duration
2. F_0, μ_2 that concern the way the random-walk is biased and impacts the appearance of recurrent communities
3. L , the box size, tuned to reproduce the average degree.

The contact duration contrast for each pair is defined by

$$\delta_i = t_i / \bar{t}, \quad (2)$$

so that the contact duration t_i is a first essential ingredient. The mean interaction time is

$$\bar{t} = w / N_{int} \quad (3)$$

so that the weight w and the number of interaction N_{int} (between the 2 individuals) are also important.

In the following we have focused on the *hosp* dataset provided by the authors.

We have run the model (10 simulations each time) with the base parameters which are $\mu_1 = 0.8, \mu_2 = 0.9, F_0 = 0.12$.

We noticed that the tail of the contact duration does not match well the data as shown in Figure 13(a). This is also apparent in the Supplementary Material of [7] (Fig. 7(a)) but somewhat hidden by the logarithmic binning (see paper Sect. I.B). We have looked for a better μ_1 value and found that $\mu_1 = 0.7$ gives a better agreement for the contact duration but rather in the intermediate values range. The other relevant distributions Figure 13(b-d) are not very satisfactory and our adjustment for μ_1 has finally little impact on the resulting contrast distribution Figure 13(e).

We have also tried varying the F_0 and μ_2 parameters but none of the results were more satisfactory (we did not change L since getting a correct average degree is an essential feature).

Overall we noticed that the contrast distribution is very robust to any change of the parameters and can hardly be modified in the default setup.

Each agent in the model is assigned an activity number r_i , which gives the probability to go from an inactive state to an active one. It is sampled uniformly by default between 0 and 1. We have tried instead to set this probability to some fixed values but again the contrast distribution varied very little.

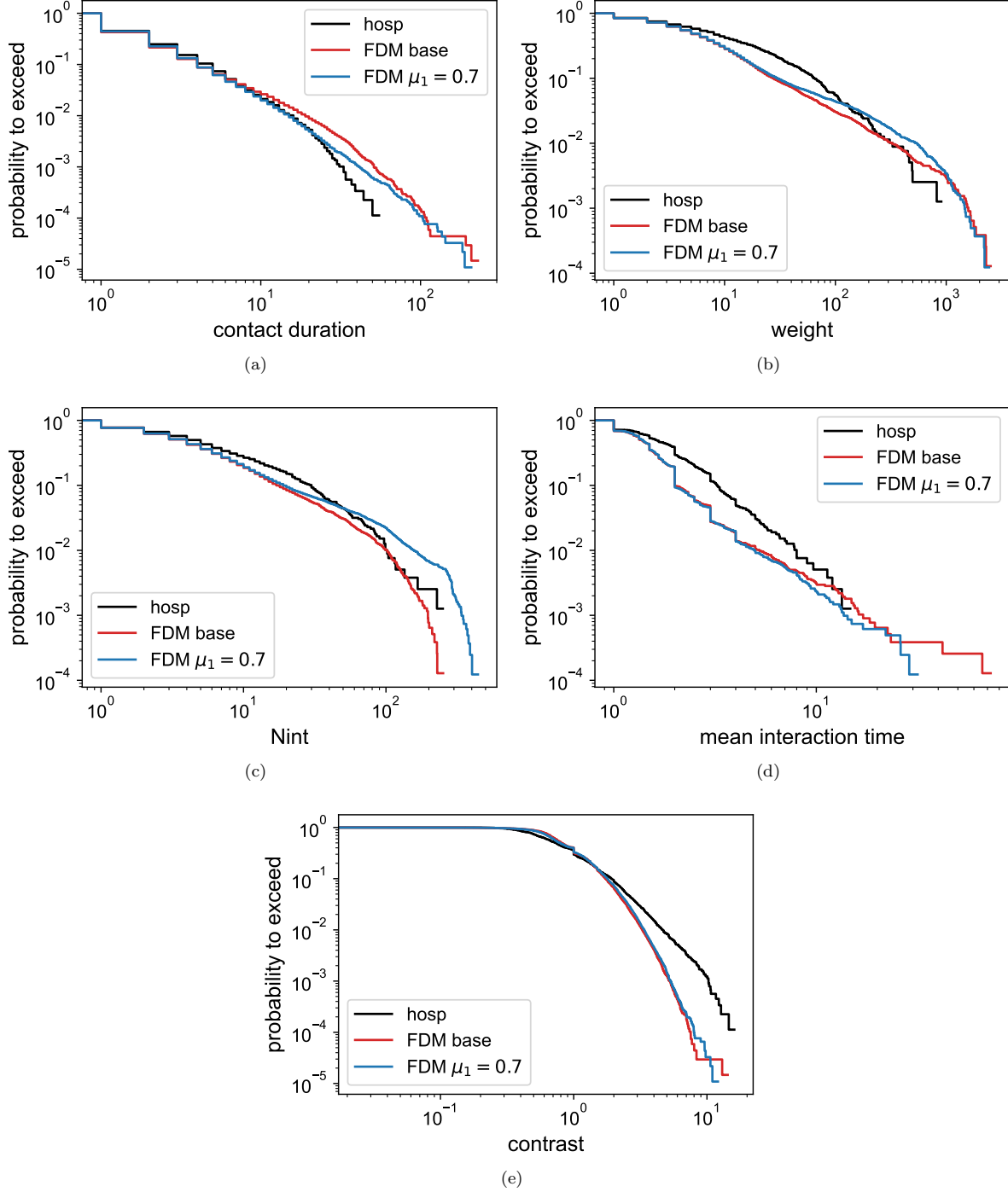


Figure 13: Distributions (p.t.e) of (a) the overall contact duration, (b) the weights (i.e the sum of the duration of contacts for each pair), (c) the number of contacts between each pair, (d) their mean interaction time and (e) the duration contrast. The black lines are obtained with the (*hosp*) data, the red ones with the base FDM implementation and the blue ones with the adjusted FDM model $\mu_1 = 0.7$.

References

- [1] Ciro Cattuto, Wouter Van den Broeck, Alain Barrat, Vittoria Colizza, Jean-François Pinton, and Alessandro Vespignani. Dynamics of Person-to-Person Interactions from Distributed RFID Sensor Networks. *PLoS ONE*,

5(7):e11596, July 2010.

- [2] Juliette Stehlé, Nicolas Voirin, Alain Barrat, Ciro Cattuto, Vittoria Colizza, Lorenzo Isella, Corinne Régis, Jean-François Pinton, Nagham Khanafer, Wouter Van den Broeck, and Philippe Vanhems. Simulation of an SEIR infectious disease model on the dynamic contact network of conference attendees. *BMC Medicine*, 9(1):87, December 2011.
- [3] Mathieu Génois, Christian L. Vestergaard, Julie Fournet, André Panisson, Isabelle Bonmarin, and Alain Barrat. Data on face-to-face contacts in an office building suggest a low-cost vaccination strategy based on community linkers. *Network Science*, 3(3):326–347, September 2015.
- [4] Mathieu Génois and Alain Barrat. Can co-location be used as a proxy for face-to-face contacts? *EPJ Data Science*, 7(1):11, May 2018.
- [5] Julie Fournet and Alain Barrat. Contact Patterns among High School Students. *PLoS ONE*, 9(9):e107878, September 2014.
- [6] Rossana Mastrandrea, Julie Fournet, and Alain Barrat. Contact patterns in a high school: A comparison between data collected using wearable sensors, contact diaries and friendship surveys. *PLoS ONE*, 10(9):e0136497, 09 2015.
- [7] Marco Antonio Rodríguez Flores and Fragkiskos Papadopoulos. Similarity Forces and Recurrent Components in Human Face-to-Face Interaction Networks. *Physical Review Letters*, 121(25):258301, December 2018.